A Biosensing Soft Robot: Autonomous Parsing of Chemical Signals through Integrated Organic and Inorganic Interfaces

Kyle B. Justus[1], Tess Hellebrekers[2], Daniel Lewis[3], Adam Wood[1], Christian Ingham[1], Carmel Majidi[1,3,4,*], Philip R. LeDuc[1,4,*], Cheemeng Tan[2,*]

[1] *Department of Mechanical Engineering, Carnegie Mellon University, Pittsburgh PA 15213*

[2] *Robotics Institute, Carnegie Mellon University, Pittsburgh PA 15213*

[3] *Department of Biomedical Engineering, University of California, Davis, Davis CA 95616*

[4] *Department of Biomedical Engineering, Carnegie Mellon University, Pittsburgh PA 15213*

*corresponding authors: Carmel Majidi (cmajidi@andrew.cmu.edu), Philip LeDuc (prl@andrew.cmu.edu), and Cheemeng Tan (cmtan@ucdavis.edu)

The integration of synthetic biology and soft robotics can fundamentally advance sensory, diagnostic, and therapeutic functionality of bio-inspired machines. However, such integration is currently impeded by the lack of soft-matter architectures that interface synthetic cells with electronics and actuators for controlled stimulation and response during robotic operation. Here, we synthesize a soft gripper that uses engineered bacteria for detecting chemicals in the environment, a flexible LED circuit for converting biological to electronic signals, and soft *pneu-net* actuators for converting the electronic signals to movement of the gripper. We show that the hybrid bio-LED-actuator module enables the gripper to detect chemical signals by applying pressure and releasing the contents of a chemical-infused hydrogel. The bio-hybrid gripper uses chemical sensing and feedback to make actionable decisions during a pick-and-place operation. This work opens new avenues in soft materials, synthetic biology, and integrated interfacial robotic systems.

INTRODUCTION

The next generation of soft robotic systems will be tremendously enhanced by integrating synthetic biology and soft materials. Synthetic biology allows the development of bio-inspired architectures that enable the integrated functionality of biological systems across different length-scales. Such advancements complement recent progress in soft robotics, which utilizes soft materials in order to achieve compliant, lightweight, and multifunctional systems that match the

robust mechanical properties and rich versatility of natural biological tissues and organisms (*1-7*). To date, the building blocks of these soft robots have largely been limited to material architectures composed of elastomers, fluids, metal alloys, and other inorganic matter. These include *artificial muscle* actuators that use pneumatics, shape memory alloy, dielectric elastomers, and a variety of other methods for robot limb motion (*3*), and *artificial skin* technologies that are capable of mechanically robust sensing and circuit wiring (*2*), and color change through microfluidics (*8*), chemical stimulation (*9*), or electroluminescence (*10*). At the systems-level, soft and elastic materials have been utilized to create biologically-inspired robots that mimic natural organisms (*11-16*) and bioinspired grippers (*17, 18*). Recently, there have been efforts to combine soft materials with natural cells to create "bio-hybrid" systems that respond to external stimuli. Examples include swimming and crawling bio-hybrid robots that are powered by contractile cells cultured on a polydimethylsiloxane (PDMS) substrate (*19, 20*) or 3D printed scaffold (*21*). By reprogramming the inner workings of cells to exploit their inherent versatility, researchers have also created microscale machines capable of functioning as sensors, computational tools, and timekeeping devices (*22-27*). The resulting synthetic biological systems allow for miniaturization of versatile chemical-signal detection. Together, these properties make synthetic cells promising candidates as sub-components within an integrated, flexible, bio-inspired structure for applications in soft robotics or wearables (*28*). The successful implementation of synthetic biological systems within flexible, soft robots has the potential to increase system functionality, as well as reduce spatial requirements for external control systems.

A fundamental challenge in integrating cells with soft robots is the lack of an interfacial module for simultaneously achieving signal exchange between the external environment and cells, communication between the cells and internal electronics, and control between the internal

electronics and host mechanics of the robot. Such an interfacial module would have to prevent the escape of the engineered cells while allowing for the exchange of chemical or electronic signals from the environment. Moreover, the module must be capable of converting these environmental signals to cellular signals and, finally, to the electronic signals. All the signal conversion must be accomplished while the module remains compliant to the flexible movement of the robot and achieve the above functions within small-scale devices.

RESULTS

To demonstrate how these challenges can simultaneously be addressed, we designed and integrated a bio-sensing module featuring genetically engineered *Escherichia coli* into soft robotic grippers that contain embedded electronics and are capable of fluidic actuation (**Figure 1A**). The basic module comprises a patterned elastomeric well that is sealed with a porous membrane to house a genetically engineered strain of *E. coli*. We selected E. coli as the chemical-sensing layer because of the flexibility for incorporating a broad range of existing synthetic genetic circuits, the modularity of adding E. coli to the soft robots, and the ability to create a new class of soft robotic sensor modality. This bacterial strain is designed to produce a genetic response to a chemical inducer in the form of a fluorescent protein which the embedded electronic components both excite and detect before distributing the information to a CPU to initiate robotic decision making and actuation. This integrated approach allows for truly autonomous robotic functionality in which grasping tasks are performed following decisions based on external stimuli that are detected and photonically transmitted by embedded synthetic cells.

Bio- Sensing Module

Before demonstrating the full soft bio-hybrid robot implementation, we first establish the integration of the cells within the soft material carrier medium used for the robot housing. We

control the interface between the external environment and the hybrid bio-LED-actuator module that allows for chemical diffusion and prevents the escape of the bacteria while maintaining the flexibility of the soft robot. We examine three membrane compositions – polyethersulfone (PES)

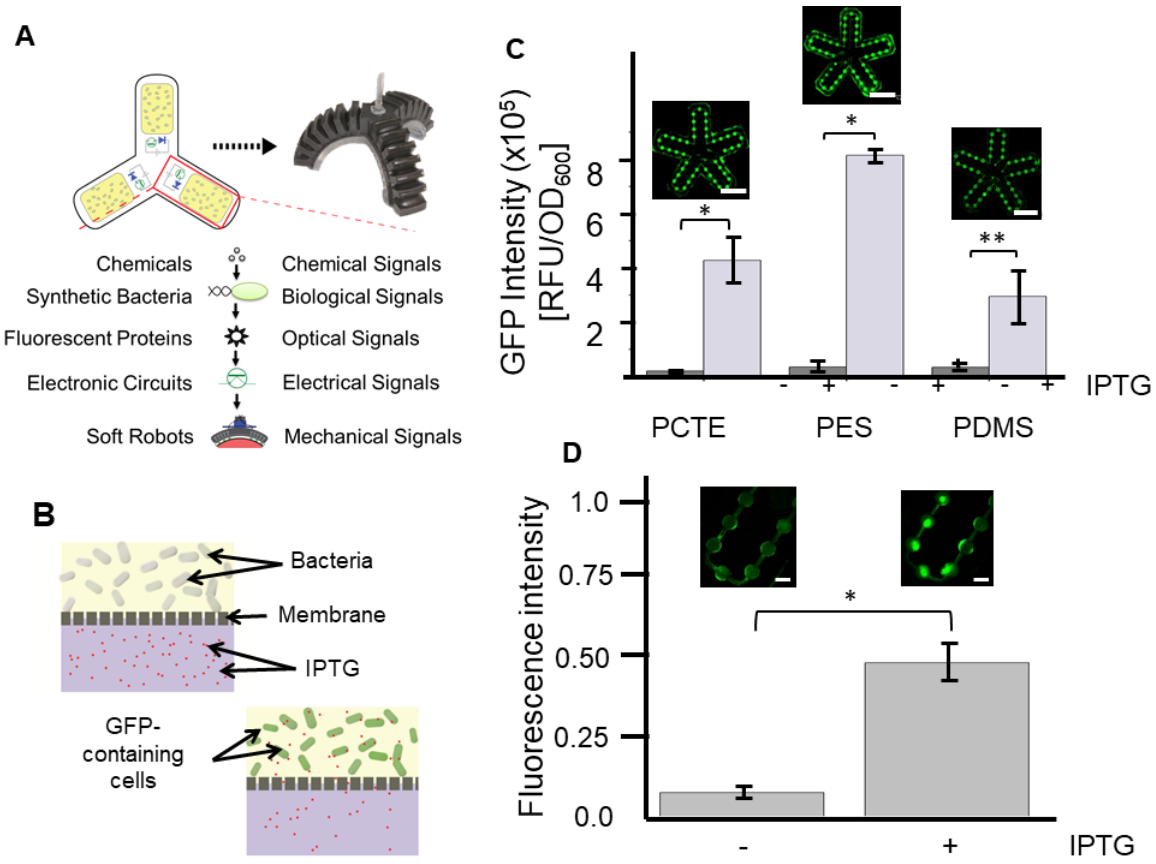

Figure 1: Integrating chemical-responsive synthetic cells and flexible materials for a biosensing soft robot. (A) Our approach integrates genetically modified *E. coli* housed in fluidic wells and channels within a PDMS polymer mold. This approach enables an integrated soft robotic system featuring pneumatic actuation and embedded electronics with feedback from engineered cells. **(B)** The sealing membranes possess pores that allow chemical stimuli while rejecting bacteria to maintain biosensing capabilities. **(C)** To have control over the engineered cell interface, various membrane compositions were integrated with the device and evaluated for permeability, including polycarbonate tracked-etched (PCTE), polyethersulfone (PES) and polydimethylsiloxane (PDMS); Scale bars, 2 cm. The level of fluorescence expression due to IPTG permeation through each membrane (PCTE (n=3), PES (n=4) and PDMS(n=4)) was measured using a plate reader. Data represents three to four replicates and SEM (*$p<0.05$, **$p<0.10$). **(D)** Induced chemo-sensitive bacteria were introduced into a patterned PDMS layer sealed by a transparent PDMS membrane and imaged using a laser scanner to observe the fluorescent signal from within the device. Scale bars, 3 mm. Normalized data represent ten measurements and SEM (*$p<0.05$).

and polycarbonate track-etched (PCTE) membranes (*29*) as well as a porous PDMS-$NaHCO_3$ membrane– by inducing cells housed within the sealed elastomeric wells (*30*). The PES and PCTE membranes provide more uniform pore sizes and distributions, but themselves lack elastomeric properties and optical transparency - properties that are achieved with the PDMS based membrane. All membranes have pore sizes less than 0.5μm diameter, which enables the retention of *E. coli* bacteria while allowing the transport of chemical stimuli into the device from the external environment (**Figure 1B**). These membranes retain the bacteria in the patterned wells of the PDMS biolayer. The permeability of each membrane is measured using IPTG-sensitive bacteria and fluorescence microspheres as controls to examine the effectiveness of each membrane (**Figure 1C**). All three membrane materials demonstrate the diffusion of fluorescent dye into the device wells, supporting all three as viable components within the device design. Due to the position of the membrane relative to the pneu-net actuators, PES and PCTE membranes can be utilized in this device despite lacking elastomeric properties as they are located in the strain-limiting layer and are not required to stretch during gripper motion.

Beneath the membranes that allow the exchange of chemicals, we incorporate a flexible PDMS layer using 3D-printed molds for housing synthetic bacteria. The wells and channels within this layer are then sealed with the membrane, and synthetic bacteria are delivered through the liquid media via fluidic channels. Next, we examine the patterned well geometries regarding growth and optical performance using bacteria that carry a chemically-inducible pIV_GFP genetic module (*31*) that expresses a green fluorescent protein (GFP). The growth of the genetically engineered bacteria in four distinct geometries of constant volume (circular, rhombic, square, and ellipsoidal patterns) are measured and found to produce minimal effects on bacterial proliferation (**Supplementary Figures S1 & S2**). Furthermore, log phase bacteria are induced with IPTG and

introduced into the embedded wells and then cultured for at least 4 hours. The resulting GFP intensities of the synthetic bacteria yield an approximately 500% increase in normalized fluorescence **(Figure 1D)**.

LED Integration

Embedded electronics are required to transmit signals from the cell (e.g., fluorescent signaling) to the soft robot CPU and controller. Both the membrane and the cell chamber constitute the bio-layer that allows the bacteria to detect and respond to chemicals in the environments. To convert the biological signal to an electronic signal, we implement an onboard and centimeter scale circuit to convert fluorescence signals from bacteria to electrical signals for the first time. The output fluorescence of the bacteria requires both an excitation wavelength and emission detector. Therefore, we validate that onboard LEDs are sufficient to excite fluorescent proteins, and then introduce a photodetector to measure the output fluorescence.

To accomplish this, we embed LEDs within the elastomer substrate of the bio-layer as an excitation light source. The LEDs are powered by an off-board supply and arranged radially in the direction of the five flexible appendages comprising the soft gripper design. The bottom of the biolayer is bonded to a silicone elastomer (Ecoflex 00-30; Smooth-On Inc.) embedded within a network of inflatable air chambers (**Methods and Materials** and **Supplementary Figure S3**). Next, the bio-layer is filled with IPTG-induced *E. coli* that have synthesized GFP. The GFP within the wells is then excited by the embedded LED circuit near the excitation peak and observed using a series of glass filters and a wide-field stereomicroscope (**Figure 2A**, LED circuit removed from composite in image processing; raw images in **Methods and Materials** and **Supplementary Figures S4** & **S5**). Induced cells within the system produce a fluorescence expression level of

approximately 400% of uninduced and unmodified *E. coli* (**Figure 2B, Methods and Materials** and **Supplementary Figure S4**). We also show that the light source can activate an optogenetic circuit of bacteria that carry a pDusk-GFP genetic module, which expresses GFP in the absence of blue light (470nm) (*32*) (**Supplementary Figures S6, S7, S8**). The results together suggest that the onboard light source can excite fluorescent proteins or modulate the conformation of a light-responsive protein which is further demonstrated by repressing the gene expression using the module itself **(Supplementary Figure S9)**.

FlexPCB Integration

After building an interface between cell response and electronic signaling, we next integrate these cell-electronic responses into a functional soft robotic system. Building upon the excitation light source, we develop a soft electronic circuit that detects the fluorescence signals and converts it into a usable electronic signal with which to guide robotic behavior through an end-effector. To achieve the on-board detection module, we embed a flexPCB within the bio-layer (**Methods and Materials** and **Supplementary Figure S10**). The circuit places an LED and phototransistor directly below each cell chamber. A critical design challenge involves maximizing LED brightness while avoiding phototransistor saturation. In addition, the LED wavelength must sufficiently activate the fluorescent proteins with a complementary filter for the phototransistor that has a wavelength between the excitation and emission spectrum of the cell's fluorescent output. The final design uses mCherry fluorescent proteins ($\lambda_{excitation}$=587nm; $\lambda_{emission}$=610nm), an amber LED (λ_{peak}=574nm), a red filter (λ_{pass}>590nm), and phototransistor (λ_{max}=570nm). We embed the circuit into a strain-limiting PDMS layer, submerge the device in controlled aqueous solutions for chemical sensitivity conditions, and collect phototransistor data. With this optimal balance of

wavelength sensitivity and filtering, we show that this onboard circuit can differentiate between IPTG+ from control environments . Altogether, we demonstrate the detection of a genetic response and subsequent conversion into a usable electrical signal within a flexible soft robotic architecture for the first time.

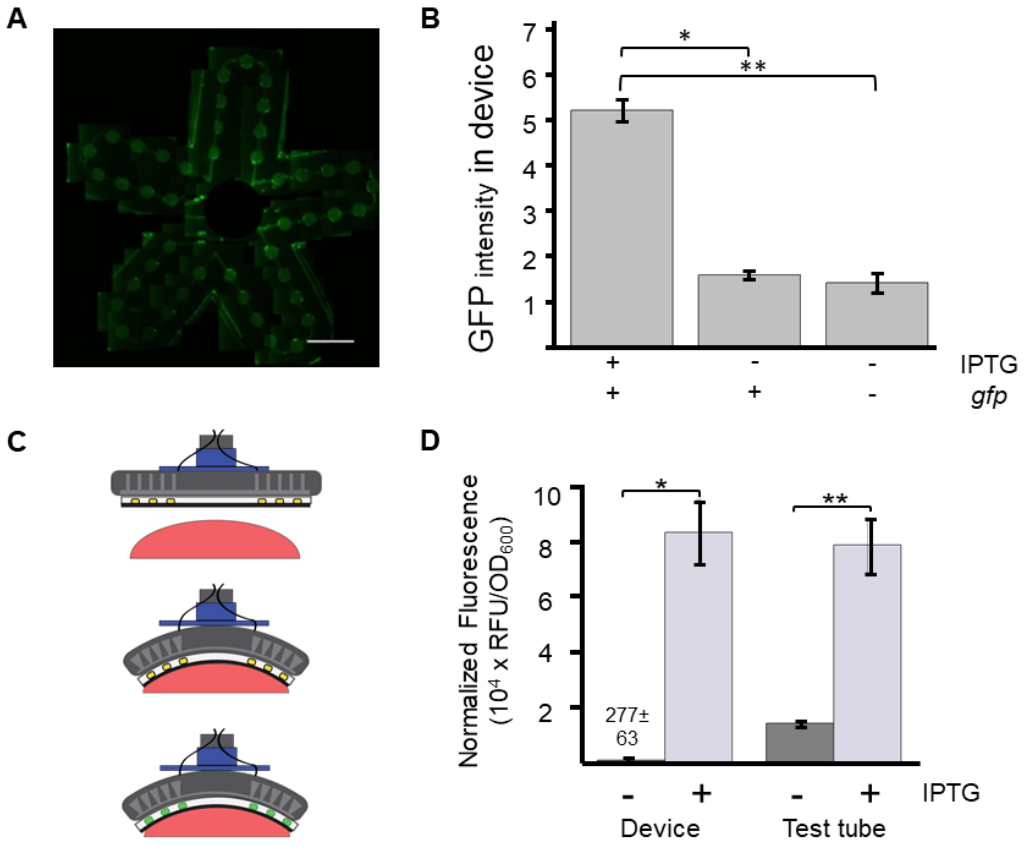

Figure 2: Establish the organic-inorganic interface of the gripper. (A) The synthetic bacteria are introduced into individual wells containing induced synthetic *E. coli*. The excitation capabilities of the embedded blue-wavelength LED circuit are tested using a stereomicroscope and a combination of filters for wide-field imaging, demonstrating the capabilities of the LED circuit to elicit a response from the contained cells. Scale bar = 10 mm **(B)** Housed within the device, induced bacteria exhibit higher fluorescence intensities than uninduced and unmodified MG1655 *E. coli*. Data represent nine measurements and SEM (*p<0.01, **p<0.01). **(C)** The sensing capabilities of the device are evaluated in an aqueous environment and chemo-sensitive cells are utilized to determine the presence of IPTG in submerged hydrogels. **(D)** The device successfully distinguished between IPTG-infused and standard hydrogels, producing a higher normalized florescence ratio between the test and control than the same strains induced in test tubes. Data represent mean ± SEM for 3 separate experiments (*p<0.05, **p<0.05).

Soft Gripper Actuation

While the hybrid bio-LED-actuator module allows us to control the biological response, the module should not interfere with the natural mechanical compliance of the host soft robot. We measure the actuation of the soft gripper with the modified bio-layer and observe the liquid media and bacteria are retained within the wells despite the deformation (**Methods and Materials** and **Supplementary Figure S11**). Based on our design configuration, the wells and bacteria are placed with the *strain-limiting layer* of the actuator, which is required for the pneu-net to bend in a preferential direction. Along with active control of the soft robotics platform, it is also essential to demonstrate environmental-sensing functionality of the integrated cellular module (**Supplemental Movie SM1**). We examine the response of our designed sensing approach using a molded hydrogel infused with the chemical stimulus IPTG while submerged in a water bath (**Figure 2C**). The device is suspended via pneumatic tubing within an incubator at 30° C, and slowly lowered until the center of the device contacts the hydrogel. Next, the pressure in the pneu-net channels is increased to initiate contact between the membrane-sealed surface of the device and the submerged hydrogel. After the contact, the relative fluorescence intensities of the device interacting with an IPTG hydrogel are almost 300 times higher than negative controls lacking IPTG, performing as well as the bacteria in test tubes (**Figure 2D**). The results indicate that the chemo-sensing bacteria within the device are integrated to respond to environmental cues from external environments within our soft robotic system.

Integrated Soft Robot Gripper

Combining our advances, we demonstrate a soft robotic decision-making system that detects and responds to an environmental chemical signal. To accomplish this, we combine the bio-layer, flexPCB, and pneunets to create a biogripper that is mounted to a 4-DOF robotic arm, where it can interact with an incubated media bath (**Figure 3A & 3B, Materials & Methods,** and **Supplementary Figures S12** & **S13**). The circuit samples the fluorescent output of the cells and stores the data. The robot arm is programmed to raise the device during the sampling period and lower the biogripper into the bath between samples to avoid reflective noise from the bath. After the sampling, the device can detect the genetic response induced by the presence of IPTG (**Figure 3C, Supplementary Figures S10** & **S14**). We use these results to calibrate a threshold-based control program for a pick-and-place scenario. Depending on the voltage trend collected during the experiment, the system reacts based on our programmed modules: if the bath is found to contain IPTG, the object is not deployed, and the operator is alerted; if the bath is found not to contain IPTG, the arm picks up the object and places it into the bath (**Figure 3D, Supplementary Movie SM2**).

DISCUSSION

We have successfully implemented an embedded bio-sensing module within a soft robotic testbed capable of utilizing genetically engineered cells to detect and respond to external chemical stimuli and then detecting the genetic response to inform robotic behavior. By integrating synthetic bacteria into a soft robotic system, we demonstrate the ability to expand the functionality of flexible devices through the utilization of existing biological architectures. The inclusion of synthetic bacteria as sensing mechanisms exploits the inherent abilities of cellular-level biological

systems to respond to a variety of stimuli at a low spatial cost. The combination of fluidic channels and wells with microfilter membranes allows for the retention of sensory bacteria, as well as the interaction between the synthetic cells and both chemical and optical cues. Along with broader materials selection, this fluidic functionality allows for a versatile and flexible device capable of engaging and responding to foreign objects in an aqueous environment.

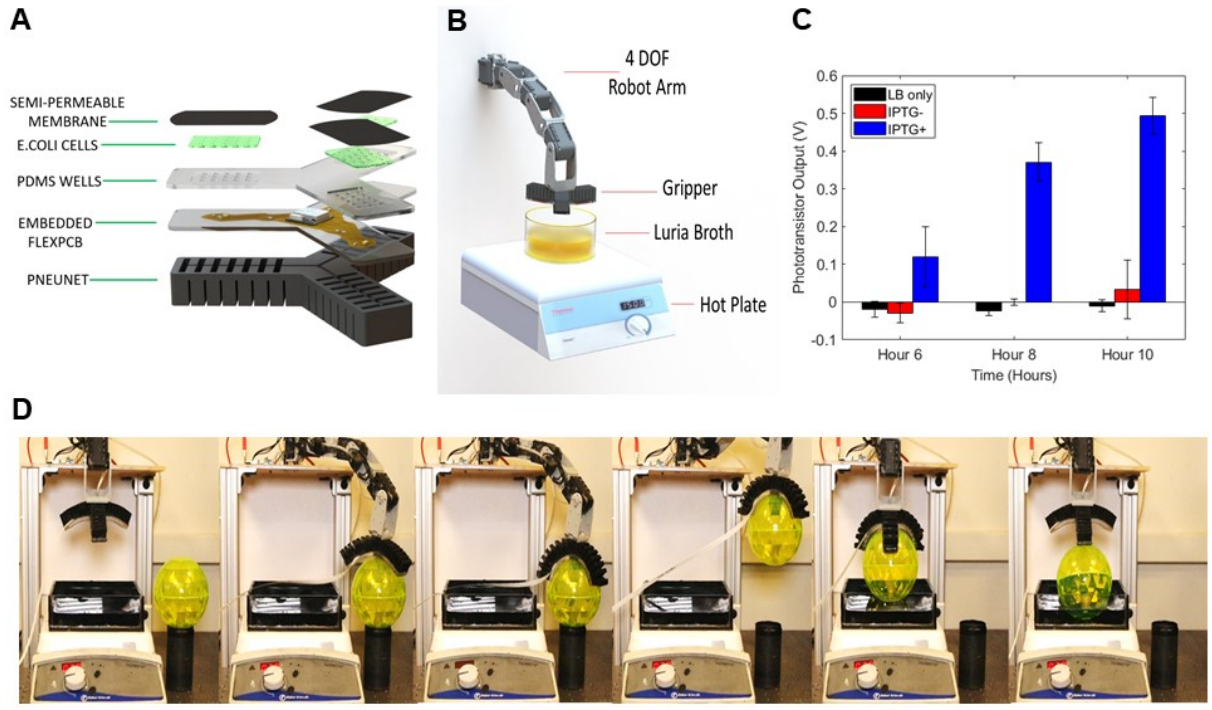

Figure 3. Robotic sorting using a soft bio-sensing gripper. **(A)** The components of the biosensing soft gripper features FlexPCB and embedded phototransistors in addition to the previously tested components. **(B)** The set-up features an incubated media bath into which the gripper is submerged via a 4-DOF robotic arm to test for sensing modality for chemical inducers. **(C)** Phototransistor output over time for IPTG+ bath with cells in the device varies significantly over time in comparison to control cases, allowing the system to make decisions based on the genetic response of the cells. Errors bars represent standard error, each data point represents average of three experiments. $P < 0.05$ for IPTG+ bath with cells against both groups. **(D)** The soft-robot sorts an object based on the phototransistor signal using the 3-finger biogripper deploying the object into a bath after classifying the bath as IPTG.

Our purpose in adopting a multi-step approach to sensing was to demonstrate that it is possible to combine synthetic biology, flexible electronics, and soft robotic actuation into a single, integrated architecture. We selected IPTG and engineered E.coli because their properties and

interactions are well understood in the existing context of synthetic biology. In this respect, they are intended to function as a model system (or surrogate) for a much wider range of chemo-bio-photonic processes that would be enabling in future applications. More generally, they demonstrate the ability to broaden the scope of soft robotic sensing to include novel biohybrid modalities that are possible with synthetic biology.

Future efforts will extend this work by creating stable hybrid organic-inorganic systems akin to the coexistence of the microbiome in the human body. Such systems will incorporate soft robotic biosensing into human-compatible soft machines and expand the complexity of signal processing by the synthetic cells. Moreover, further progress in synthetic biology will enable a wider range of chemical sensing modalities as well as improvements in sensing performance. This includes enhancements in sensing speeds as well as the use of synthetic pathways that use protein-based networks.

Methods & Materials

Biological components: The *Escherichia coli* BL21(DE3) was used to create z-competent cells before transformation. The plasmid *pIV_GFP* was created in a previous work (*1*) and inserted into cells to allow for synthesis of GFP. This plasmid was designed to initiate transcription of the *gfp* gene in presence of the chemical stimulus isopropyl β-D-1-thiogalactopyranoside (IPTG).

Constructing Optogenetic Plasmid: To construct a plasmid capable of changing gene expression in response to blue light, we digested the pDusk plasmid (Addgene 43795) with SalI and NotI, ligated in a PCR fragment containing GFP, and transformed the assembled vector into Top10 cells. Variants of pDusk_GFP, pDusk_v37_GFP and pDusk_v38_GFP were made by changing the ribosome binding site. The ribosome binding site was manipulated by annealing two short

single stranded DNA oligomers together to form an insert with a new RBS, then phosphorylating the insert, and ligating the insert with the vector at the XbaI and SalI sites.

Growth rate detection: The growth rate of the bacteria within the device was measured through a Beckman Coulter DU730 UV-vis spectrophotometer (Beckman Coulter, Brea, CA, USA). Optical density measurements at 600nm wavelengths were recorded before the introduction of the bacteria to the device and after subsequent growth in an incubated shaker (37 °C).

Protein expression measurement: The fluorescence intensity of reporter proteins was measured using a Tecan Infinite M1000 plate reader (Tecan, Mannedorf, Switzerland). Fluorescence intensities were normalized by optical density measurements to obtain average intensity per cells.

Culture well fabrication: The culture wells were created using a negative plastic master mold via 3D printing (Stratasys, Eden Prairie, MN) due to the deep feature depths, which are more difficult to achieve with traditional photolithography approaches. Desired molds were produced using SolidWorks (Dassault Systemes SolidWorks Corporation, Waltham, MA) and imported to the Objet printing set-up where the molds were then formed with VeroWhite printing material. The molds were then baked at 60°C for 4 hours to remove residue solvents, which can inhibit the curing of PDMS. PDMS was mixed at a 10:1 base-to-curing agent ratio and poured into the 3D printed master molds before desiccation for 45 minutes. The PDMS-filled molds were then transferred to an oven at 60°C for at least 2 hours until fully cured. Last, the PDMS layers were removed from the mold using an X-acto knife and excess PDMS was removed.

Electronics integration: An LED circuit was designed featuring 3 or 5 LEDs (depending on the gripper configuration) with a peak wavelength of 465 nm and gull wing leads (Kingbright, City of Industry, CA) all arranged in series in a compact, circular pattern. The LEDs were soldered together and connected to a copper wire lead to which an external DC power supply was connected. Once the circuit was completed, it was placed centrally within uncured PDMS deposited in the 3D printed negative mold of the fluidic channels and culture wells.

Porous membrane fabrication: Through similar work by Jiao et al (*2*), porous PDMS membranes were created via *in situ* reaction. The Sylgard 184 curing agent was mixed with sodium bicarbonate powder at a 1:1 mass ratio and mixed thoroughly before setting for 1 hour. The two materials were mixed once again before mixing with the Sylgard 184 base agent at a 1:5 mass ratio and desiccating for 20 minutes. The prepolymer-sodium bicarbonate mixture was then deposited on 120°C heat release tape at a thickness of 100 μm via thin film applicator. The PDMS was then cured at 60°C in an oven for at least 2 hours. The cured membranes were then submerged in a bath of 13M HCl plus Triton X-100 (100X dilution) for 1 hour before being thoroughly washed with water and allowed to dry in an oven at 60°C (2-4 hours).

Device assembly: The device was comprised of two main layers, one containing the biological components and the other housing the electronic components. First, 25g of PDMS prepolymer was poured into a negative mold possessing the features of the fluidic channels and bacterial growth wells. A series of blue wavelength LEDs were then placed in the center of the PDMS layer and allowed to partially cure on a hot plate. Once partially cured (25 mins @ 70°C on a hot plate), a fully cured EcoFlex layer possessing pneumatic channels (achieved through 3D printed negative

mold) was placed on top of the PDMS layer and allowed to adhere and seal off the interior channels. Following this curing process, the PDMS-EcoFlex device was carefully removed from the fluidic channel mold and the biolayer interface was then sealed off with a microfilter membrane (PDMS-$NaHCO_3$, polycarbonate or polyethersulfone) via plasma oxidation. Polycarbonate track etched (PCTE) and polyethersulfone (PES) membranes were purchased from Sterlitech with pore sizes of 0.2 μm (PCTE and PES) and 0.4 μm (PCTE). PES membranes were adhered to the PDMS biolayer component via an APTES pretreatment process outlined by Aran et al. (*3*) while the PCTE membranes were adhered using a combination of an APTES approach and sealing the membrane edges using PDMS prepolymer before curing to prevent delamination.

Permeability: Permeability of the membrane to IPTG was measured using multiple methods to verify molecular transport through the transmembrane pores. As an initial validation, membranes were suspended across microchannels (500μm width), which were formed as PDMS negative molds from 3D printed masters, and sealed using plasma oxidation. Following sterilization with 70% ethanol and UV radiation, fluorescent beads (1μm diameter) in LB media were introduced into the upper channel while sterile LB media was flowed into the lower channel, separated by the membrane. The two fluids were left to sit statically in the channels for 2 hours before fluorescent measurements using a plate reader were performed and compared with initial fluorescent readings of each solution.

Stereomicroscopy: A digital charge-coupled device (CCD) camera (The Imaging Source Europe GmbH) mounted on a stereomicroscope (SZX12, Olympus Corp., Waltham, MA) was used to perform wide-field imaging of the device to create a composite view of the LED excitation of

GFP-producing cells housed within the PDMS layers. Imaging was performed with 1X magnification with 18 V of power supplied to the 5 gull wing LEDs, while the sealed bio-layer was positioned on an actuating stage and moved accordingly during a time series capture with 3 second intervals.

Pneumatic actuation: Deflection of the device through pneumatic action within the EcoFlex layer was measured using open source motion tracking software (Tracker). Pressure was increased within the channel manually with a syringe pump and pressure levels were monitored using a piezoelectric pressure sensor (Honeywell, Morristown, NJ) interfaced with a microcontroller and MATLAB (Mathworks, Natick, MA). Pressure was increased in 0.5 psi increments from 0-5 psig. Positions were recorded along the pneumatic appendage in 0.5cm increments for each pressure step.

Hydrogel Preparation: Gelatin molds were prepared by mixing 15% w/v of gelatin from porcine skin (Sigma-Aldrich, St. Louis, MO) and heated to 80°C on a hot plate. Test samples were mixed with 1μM IPTG (Sigma-Aldrich) before being left to cool in the plastic mold.

Hydrogel sensing test: Overnight cultures of bacteria were prepared in 3mL volumes of LB with 1 μL of 50 μg/mL stock ampicillin before placing on a shaker table at 37 °C for 16 hours. The overnight cultures were then diluted 100X into fresh media and antibiotics, and allowed to grow on the incubated shaker table for 4 hours. The bacteria were then extracted from the test tube and injected into the fluidic reservoirs of two devices. The remaining bacteria were then split into 1 mL volumes in fresh test tubes, one of which was induced with IPTG (1mM). The two devices

were placed in incubators at 30°C. One was brought into contact with an IPTG infused gelatin mold submerged in LB while the other was brought into contact with a standard gelatin mold submerged in LB. The pneu-net channels of the devices were activated in parallel using syringes and tubing fixed within a quick-clamp to insure constant pressure. The devices were left in place for 4 hours before extraction via syringe. The samples were then measured using an absorbance and fluorescence plate reader (Tecan, Mannëdorf, Switzerland) along with the samples from the test tubes.

Plate Reader Comparison: The **Supplementary Table S1** compares the phototransistor output, in volts, to the RFU output for the mCherry genetic constructs in BL21DE3 cells, dimensionless, from the fluorescence plate reader (Tecan, Mannedorf, Switzerland). The cells were tested under mCherry conditions with an excitation frequency of 587 nm and emission frequency of 610 nm.

Author contribution

KJ, TH, CM, PL, and CT wrote the manuscript. PL and CT conceived the work. PL, CM, TH, and KJ designed the soft material systems. DL and CT designed the synthetic cells. KJ, TH, AW, CI, and DL performed the experiments.

Acknowledgements

We thank S. Saurabh, J. Wissman, M. Hazar and E. Parigoris for assistance. This work is supported by an industry/campus supported fellowship under the Training Program in Biomolecular Technology (T32-GM008799) (DL), the Branco-Weiss Fellowship (CT), Human Frontier Science Program (CT), National Science Foundation (CBET-1547810, PL; CHE 1808237, CT), and the Air Force Office of Scientific Research (FA9550-13-1-01 08, PL). T.H. and C.M. acknowledge support from the Office of Naval Research (Grant #N000141612301; PM: Dr. Tom McKenna; Bio-Inspired Autonomous Systems).

References

1. S. Bauer *et al.*, 25th anniversary article: A soft future: from robots and sensor skin to energy harvesters. *Adv Mater* **26**, 149-161 (2014).
2. M. L. Hammock, A. Chortos, B. C. K. Tee, J. B. H. Tok, Z. A. Bao, 25th Anniversary Article: The Evolution of Electronic Skin (E-Skin): A Brief History, Design Considerations, and Recent Progress. *Adv Mater* **25**, 5997-6037 (2013).

3. F. Ilievski, A. D. Mazzeo, R. F. Shepherd, X. Chen, G. M. Whitesides, Soft robotics for chemists. *Angew Chem Int Ed Engl* **50**, 1890-1895 (2011).
4. S. Kim, C. Laschi, B. Trimmer, Soft robotics: a bioinspired evolution in robotics. *Trends Biotechnol* **31**, 287-294 (2013).
5. S. I. Rich, R. J. Wood, C. Majidi, Untethered soft robotics. *Nature Electronics* **1**, 102-112 (2018).
6. D. Rus, M. T. Tolley, Design, fabrication and control of soft robots. *Nature* **521**, 467-475 (2015).
7. M. Wehner *et al.*, An integrated design and fabrication strategy for entirely soft, autonomous robots. *Nature* **536**, 451-455 (2016).
8. S. A. Morin *et al.*, Camouflage and Display for Soft Machines. *Science* **337**, 828-832 (2012).
9. G. R. Gossweiler *et al.*, Mechanochemically Active Soft Robots. *ACS Appl Mater Interfaces* **7**, 22431-22435 (2015).
10. C. Larson *et al.*, Highly stretchable electroluminescent skin for optical signaling and tactile sensing. *Science* **351**, 1071-1074 (2016).
11. M. Calisti *et al.*, An octopus-bioinspired solution to movement and manipulation for soft robots. *Bioinspir Biomim* **6**, 036002 (2011).
12. M. Cianchetti, M. Calisti, L. Margheri, M. Kuba, C. Laschi, Bioinspired locomotion and grasping in water: the soft eight-arm OCTOPUS robot. *Bioinspir Biomim* **10**, 035003 (2015).
13. H. T. Lin, G. G. Leisk, B. Trimmer, GoQBot: a caterpillar-inspired soft-bodied rolling robot. *Bioinspir Biomim* **6**, (2011).
14. R. V. Martinez *et al.*, Robotic tentacles with three-dimensional mobility based on flexible elastomers. *Adv Mater* **25**, 205-212 (2013).
15. K. Suzumori, S. Endo, T. Kanda, N. Kato, H. Suzuki, A Bending Pneumatic Rubber Actuator Realizing Soft-bodied Manta Swimming Robot. *Proceedings of the IEEE International Conference of Robotics and Automation (ICRA)*, (2007).
16. C. L. Zhou, K. H. Low, Design and Locomotion Control of a Biomimetic Underwater Vehicle With Fin Propulsion. *Ieee-Asme T Mech* **17**, 25-35 (2012).
17. R. Deimel, O. Brock, A novel type of compliant and underactuated robotic hand for dexterous grasping. *Int J Robot Res* **35**, 161-185 (2016).
18. X. C. Zhou, C. Majidi, O. M. O'Reilly, Soft hands: An analysis of some gripping mechanisms in soft robot design. *Int J Solids Struct* **64-65**, 155-165 (2015).
19. A. W. Feinberg *et al.*, Muscular thin films for building actuators and powering devices. *Science* **317**, 1366-1370 (2007).
20. J. C. Nawroth *et al.*, A tissue-engineered jellyfish with biomimetic propulsion. *Nat Biotechnol* **30**, 792-797 (2012).
21. C. Cvetkovic *et al.*, Three-dimensionally printed biological machines powered by skeletal muscle. *P Natl Acad Sci USA* **111**, 10125-10130 (2014).
22. T. L. Deans, A. Singh, M. Gibson, J. H. Elisseeff, Regulating synthetic gene networks in 3D materials. *P Natl Acad Sci USA* **109**, 15217-15222 (2012).
23. Y. Ding, F. Wu, C. Tan, Synthetic Biology: A Bridge between Artificial and Natural Cells. *Life (Basel)* **4**, 1092-1116 (2014).
24. M. B. Elowitz, S. Leibler, A synthetic oscillatory network of transcriptional regulators. *Nature* **403**, 335-338 (2000).

25. A. S. Khalil, J. J. Collins, Synthetic biology: applications come of age. *Nat Rev Genet* **11**, 367-379 (2010).
26. C. M. Tan, S. J. Lo, P. R. LeDuc, C. M. Cheng, Frontiers of optofluidics in synthetic biology. *Lab Chip* **12**, 3654-3665 (2012).
27. C. M. Tan, S. Saurabh, M. P. Bruchez, R. Schwartz, P. LeDuc, Molecular crowding shapes gene expression in synthetic cellular nanosystems. *Nat Nanotechnol* **8**, 602-608 (2013).
28. X. Liu *et al.*, Stretchable living materials and devices with hydrogel-elastomer hybrids hosting programmed cells. *Proc Natl Acad Sci U S A* **114**, 2200-2205 (2017).
29. K. Aran, L. A. Sasso, N. Kamdar, J. D. Zahn, Irreversible, direct bonding of nanoporous polymer membranes to PDMS or glass microdevices. *Lab Chip* **10**, 548-552 (2010).
30. K. X. Jiao, C. L. Graham, J. Wolff, R. G. Iyer, P. Kohli, Modulating molecular and nanoparticle transport in flexible polydimethylsiloxane membranes. *J Membrane Sci* **401**, 25-32 (2012).
31. M. I. Lebedeva, E. V. Rogozhkina, N. A. Tsyba, S. V. Mashko, A New T7 Rna Polymerase-Driven Expression System Induced Via Thermoamplification of a Recombinant Plasmid Carrying a T7 Promoter Escherichia-Coli Lac Operator. *Gene* **142**, 61-66 (1994).
32. R. Ohlendorf, R. R. Vidavski, A. Eldar, K. Moffat, A. Moglich, From Dusk till Dawn: One-Plasmid Systems for Light-Regulated Gene Expression. *J Mol Biol* **416**, 534-542 (2012).